Available online at www.sciencedirect.com
SCIENCE DIRECT
Polymer 46 (2005) 7403–7409
polymer
www.elsevier.com/locate/polymer

# Melt intercalation of poly(L-lactide) chains into clay galleries

Pham Hoai Nam, Masahiro Kaneko, Naoya Ninomiya, Atsuhiro Fujimori, Toru Masuko*

*Department of Polymer Science and Engineering, Faculty of Engineering, Yamagata University, Jonan 4-3-16, Yonezawa, Yamagata 992-8510, Japan*

Received 24 February 2005; received in revised form 6 June 2005; accepted 14 June 2005
Available online 19 July 2005

**Abstract**

The melt intercalation of poly(L-lactide) (PLLA) chains into silicate galleries has been investigated via a melting process without any shearing force at elevated temperature. Under the melting process, the incorporation of various types of organo-modified montmorillonites into PLLA matrix lead to the increase in the basal spacing of clay particles in different manner without delamination into individual layers. The changes in layer-stacked structures of the clay particles in the PLLA matrix were examined by use of wide-angle X-ray diffraction and transmission electron microscopy. The effects of clay content in PLLA matrix and clay surfactants on the melt intercalation of PLLA were discussed in terms of chain mobility.


*Keywords:* Poly(L-lactide); Montmorillonite; Intercalation

## 1. Introduction

Since the clay particles have been able to disperse uniformly in the polymer matrix in nanometer scale, the resultant polymer/clay hybrids (PCHs) exhibit remarkable enhancements in their dimensional stability, gas barrier performance, especially in mechanical properties as compared with conventional composites [1–5]. Several kinds of preparation methods for PCHs have been reported so far, such as in situ intercalative polymerization, melt-intercalation, exfoliation-adsorption, and template synthesis [3]. Of those methods, melt-intercalation has been widely used in practice due to its environmental and economical advantages.

Vaia et al. demonstrated for the first time the possibility of direct melt intercalation of polystyrene (PS) into mica galleries [6,7], where the kinetics of PS melt intercalation was examined as functions of processing temperature and molecular weight of PS. However, the effects of clay content and clay surfactants on the polymer melt intercalation have not yet been studied in detail. In order to explain the intercalating mechanism by polymer chains into clay galleries, such a profound understanding of those effects should be necessary.

Recently, we reported the uniform dispersion of clay particles in biodegradable poly(L-lactide) (PLLA) due to the good interaction between PLLA and clay [8,9]. In addition, the incorporation of several percentages of clay into PLLA did not change the original orthorhombic α-form of the PLLA matrix at all [9]. The structure and properties of PLLA/clay hybrids have also been reported elsewhere [8–12]. On the PLLA/clay hybrids, there were no studies on the mechanism of the melt intercalation of PLLA into clay galleries, although many research groups so far have been interested in sample preparation, characterization, physical properties, especially in view of their mechanical properties [13].

In this study we examine the melt intercalation of PLLA in silicate galleries for the compounds of PLLA and variously organo-modified montmorillonites (organoclays). These compounds are prepared by the melt-processing method without shearing force at elevated temperature. The changes in layer-stacked structures of organoclay during melt processing will be investigated as functions of heating time and clay content.

* Corresponding author. Tel.: +81 238 26 3071; fax: +81 238 26 3073.
*E-mail address:* tmasuko@yz.yamagata-u.ac.jp (T. Masuko).

0032-3861/$ - see front matter © 2005 Published by Elsevier Ltd.
doi:10.1016/j.polymer.2005.06.023

## 2. Experimental

The polymer used in this study was a high L-content

(>99%) commercial grade PLLA (Unitika Co. Ltd), which was dried under vacuum at 100 °C for two days and kept at room temperature in a silica gel-dried desicator for later use. Molecular characterization of PLLA was carried out on a gel permeation chromatograph (GPC: JASCO 860-CO GPC/HPLC) using tetrahydrofuran (THF) carrier at 40 °C with a flow rate of 1 ml/min. Polystyrene (PS) was utilized as the elution standard. The results were (PS-reduced) weight-average molecular weight ($M_w$) = $20\times10^4$, number-average molecular weight ($M_n$) = $10\times10^4$ and the poly-dispersity index ($M_w/M_n$) = 1.94.

Three kinds of organo-modified montmorillonite were used in this work; one was modified via cation exchange reaction with trimethyl octadecyl ammonium (clay M1), another with dimethyl dioctadecyl ammonium (clay M2), the other with bis(4-hydroxy butyl) methyl octadecyl ammonium (clay M3). The original montmorillonite has cation exchange capacity of 108.6 mequiv/100 g and its layer diameter size in range 0.2–2.0 μm. The modified clay powders were kindly supplied by Kunimine Co., Japan. The organic content in the modified clay determined by thermo-gravimetric analysis (TGA: Seiko 5200 TG/DTA) are summarized in Table. 1. The clay powders were heated to 550 °C at heating rate of 10 °C/min under an $N_2$ purge. The organic content was calculated from the residue left at 550 °C.

The compounds of PLLA and clay were prepared as following procedure. PLLA films were cut into small pieces in size about $1\times1$ mm$^2$. Both the PLLA pieces and the corresponding amount of clay were put in a small glass bottle for shaking by hand at room temperature. Concentration of clay was changed from 0 to 40 wt%. The mixture was then placed in a 1 mm thick spacer (Teflon) sandwiched between two polyimide films. The sample was melted at 190 °C in air on a hot press and then cooled down to room temperature. Note that we did not apply any shearing force to the samples. A schematic illustration of this preparation method is shown in Fig. 1. The code of the samples and their compositions are collectively listed in Table. 2.

The X-ray diffraction (XRD) profiles of the clay powder and its compounds were collected in digital data using a RAD-rA diffractometer (RIGAKU Co.) at ambient temperature. Ni-filtered Cu K$\alpha$ radiation (wavelength, $\lambda$ = 0.154 nm) was utilized at 40 kV and 100 mA. The samples were scanned in the $\theta-2\theta$ mode by use of a step-scanning method with the step-width of 0.05° and 4 s intervals in the range from $2\theta=2$ to 15°.

Table 2
Codes and compositions of the compounds used in this study

| Sample | Code | Composition (wt%) | |
|---|---|---|---|
| | | PLLA | Organoclay |
| PLLA+M1 | M11 | 95 | 5 |
| PLLA+M1 | M12 | 89 | 11 |
| PLLA+M1 | M13 | 80 | 20 |
| PLLA+M2 | M21 | 95 | 5 |
| PLLA+M2 | M22 | 89 | 11 |
| PLLA+M2 | M23 | 80 | 20 |
| PLLA+M2 | M24 | 60 | 40 |
| PLLA+M3 | M31 | 95 | 5 |
| PLLA+M3 | M32 | 89 | 11 |
| PLLA+M3 | M33 | 80 | 20 |

Alternatively, very thin films around 70 nm thick were sliced from the bulk samples at room temperature using a Reichert ultra-microtome equipped with a diamond knife. Morphological features of the dispersed clay particles in the compounds was examined by use of a transmission electron microscope (TEM, Phillips CM-300) operated at an accelerating voltage of 200 kV.

## 3. Results and discussion

### 3.1. X-ray diffraction of clay

Figs. 2–4 show the X-ray diffraction traces for the M12, M22, M32 samples, respectively, exhibiting a shift of diffraction peaks of (001) reflections towards the lower diffraction angles in different manner. We find that the (001) diffraction peaks for the sample M12 shifted from $2\theta=4.65°$ ($d_{001}=1.90$ nm) to 2.40° ($d_{001}=3.68$ nm) during a heating period for 30 s; similarly, for the sample M22 from $2\theta=2.75°$ ($d_{001}=3.21$ nm) to 2.30° ($d_{001}=3.84$ nm). On the other hand, those (001) diffraction peaks shifted in shorter range for the M32 sample. For 30 s melting process, there was only a shift from $2\theta=3.50°$ ($d_{001}=2.52$ nm) to 3.30° ($d_{001}=2.68$ nm). In addition, another peak is observed at $2\theta=2.50°$ ($d_{001}=3.53$ nm) and a shoulder at $2\theta=3.30°$ for the M32 sample melted for 1 min. This implies that only a part of (001) diffraction peak shifted to $2\theta=2.50°$ during 1 min melting process. The increase in $d_{001}$ values is probably attributed to the intercalation of PLLA chains snaking into silicate galleries. Of the PLLA/clay compounds, the M32 sample show a relatively slow shift of

Table 1
Characteristic parameters of modified clays

| Sample | Ammonium cation | Organic content in clay (wt%) | $CEC_a$[a] (mequiv/100 g) |
|---|---|---|---|
| M1 | $(CH_3)_3N^+C_{18}H_{37}$ | 25.6 | 81.90 |
| M2 | $(CH_3)_2N^+(C_{18}H_{37})_2$ | 41.4 | 75.22 |
| M3 | $(CH_3)(C_{18}H_{37})N^+(C_4H_9OH)_2$ | 37.1 | 86.59 |

[a] Apparent cation exchange degree calculated from TG/DTA results.

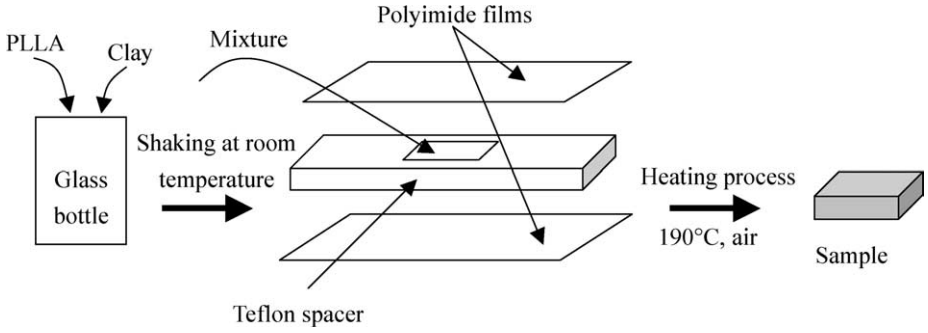


Fig. 1. Schematic illustration of sample preparation.

(001) diffraction peaks as compared with those of the M12 and M22 samples under the melting process.

After the melting process, the original (001) diffraction peaks disappeared and the new sets of (001) diffraction peaks together with (002) and (003) diffraction peaks became conspicuous for all the samples. In addition, the shapes of these peaks were not affected by the melting process. These results imply that the clay particles remain stacked regularly and their structures do not change significantly under the melting process.

### 3.2. Dependence of structural parameters of clay particles on heating time

The changes of (001) interlayer spacing of clay particles as a function of short heating time (0–5 min) is shown in Fig. 5(a)–(c) for the M1$x$ ($x$=1–3), M2$y$ ($y$=1–4), and M3$z$ ($z$=1–3) samples, respectively. Apparently, for the same heating period, the M3$z$ samples exhibited a relatively slow increase in $d_{001}$ values as compared with the others. In this case, the interaction among the hydroxy groups of ammonium surfactant, those existing in clay edges, and those of PLLA presumably retarded the penetration of PLLA chains into silicate galleries.

The changes in the $d_{001}$ values as a function of longer heating time are shown in Figs. 6–8 for the M1$x$, M2$y$, and M3$z$, respectively. We see that the $d_{001}$ values of clay particles increased with heating time and finally reached a plateau with the saturated values, $d^*_{001}$. The $d^*_{001}$ values were 3.5–3.8 nm for the M1$x$, 3.8–4.1 nm for the M2$y$, and 3.7–3.8 nm for the M3$z$ samples, seemingly to be controlled by the long alkyl chains of ammonium surfactant existing between silicate layers. Note that they were strongly dependent on clay content for the M1$x$ and M2$y$ but the M3$z$ samples. In spite of probably different mechanism of intercalation, this feature of clay in M1$x$ and M2$y$ samples is similar with that in Nylon6/clay system obtained via in situ polymerization and reported by Fukushima et al. [14].

In Figs. 6–8, the results of heating process at 190 °C in air for clay powder are also shown for comparison with those derived from clay in the compounds with PLLA. The $d_{001}$ values of clay powder changed in different manner with

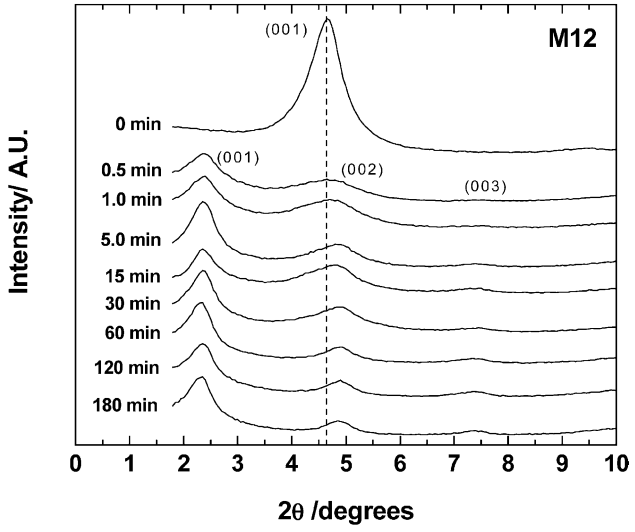


Fig. 2. WAXD traces for M12 sample melted at 190 °C for various times. The dashed lines indicate the location of silicate (001) reflection of M1 without heating process. The diffraction curves are vertically offset for clarity.

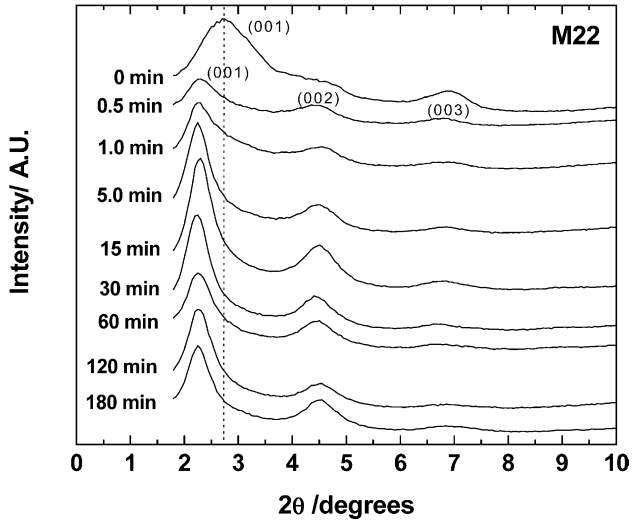


Fig. 3. WAXD traces for M22 sample melted at 190 °C for various times. The dashed lines indicate the location of silicate (001) reflection of M2 without heating process. The diffraction curves are vertically offset for clarity.

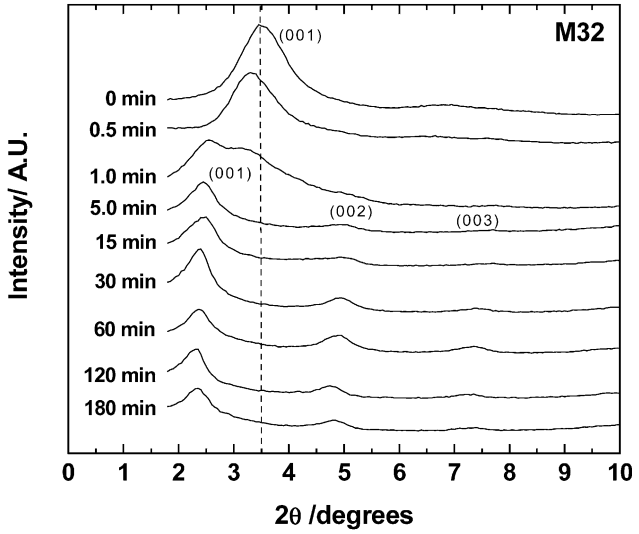


Fig. 4. WAXD traces for M32 sample melted at 190 °C for various times. The dashed lines indicate the location of silicate (001) reflection of M3 without heating process. The diffraction curves are vertically offset for clarity.

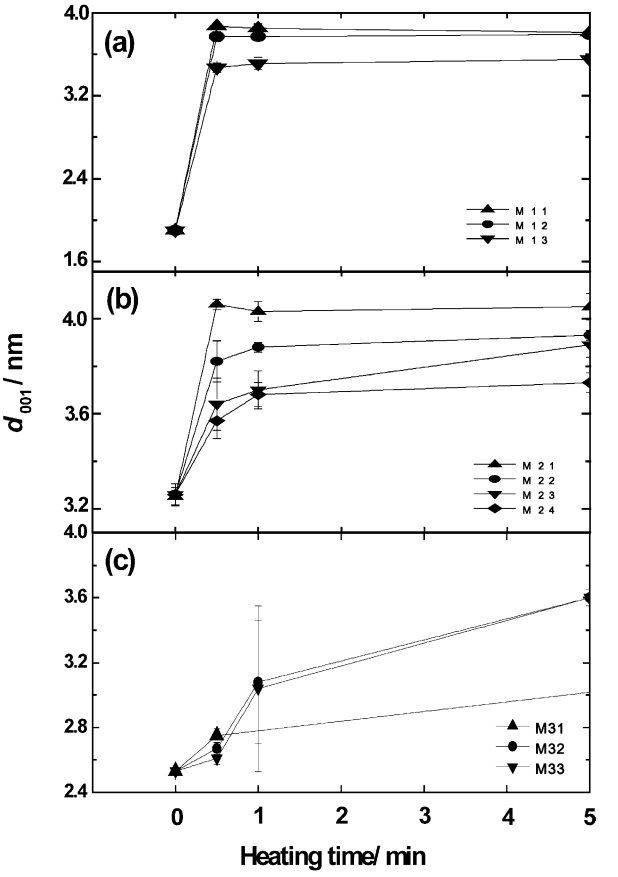


Fig. 5. Dependence of (001) interlayer spacing, $d_{001}$, of clay on short heating time for (a) M1$x$ ($x$ = 1–3), (b) M2$y$ ($y$ = 1–4), and (c) M3$z$ ($z$ = 1–3) samples.

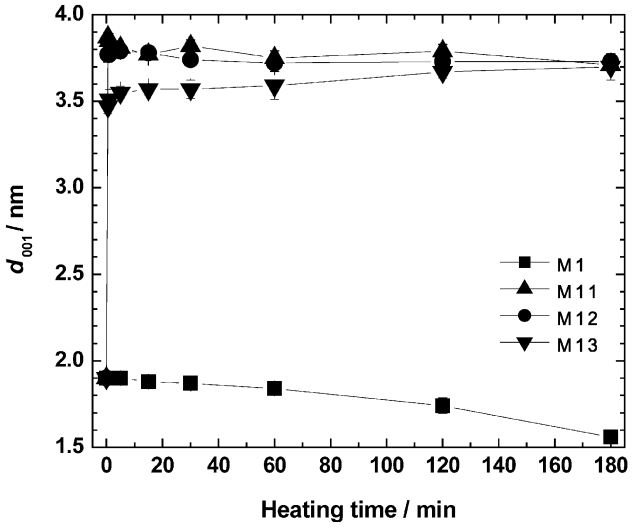


Fig. 6. Dependence of (001) interlayer spacing, $d_{001}$, of clay on heating time for M1 and M1$x$ ($x$ = 1–3) samples.

heating process. In the M1 sample, the value decreases monotonically with heating time, but increases up to various saturated levels and decreases for the M2 and M3 samples. In these cases, the increase in $d_{001}$ values is probably due to the rearrangement of alkyl chains already located within silicate galleries, while the subsequent decrease is attributed to heat degradation of the alkyl ammonium ions. The TG/DTA results (not shown here) indicate that the loss weights are about 7.6, 7.7, 5.0 wt% for M1, M2, and M3 samples, respectively, after heating process at 190 °C in air for 4 h.

The difference, $\Delta d_{001}$, between the $d_{001}$ of compounds and that of the original clay shows the value of about 1.6–1.9, 0.3–0.9 and 0.8–1.1 nm for the clay particles in M1$x$, M2$y$, and M3$z$, respectively. From the lattice dimension of the α-form of PLLA, the corresponding molecular diameter for a PLLA chain is estimated to be approximately 0.62 nm [15].

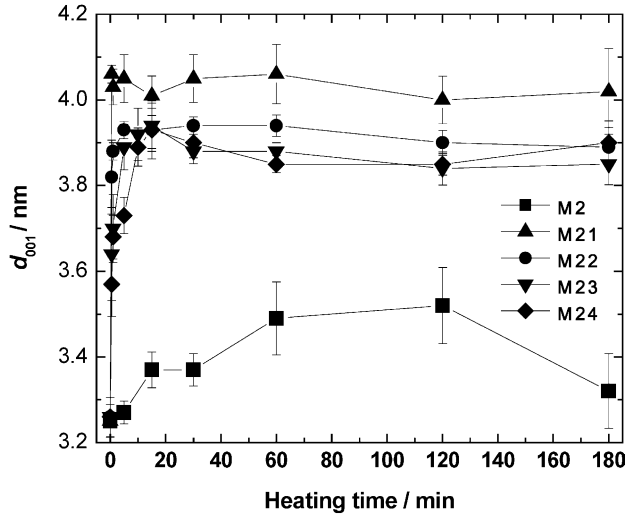


Fig. 7. Dependence of (001) interlayer spacing, $d_{001}$, of clay on heating time for M2 and M2$y$ ($y$ = 1–4) samples.

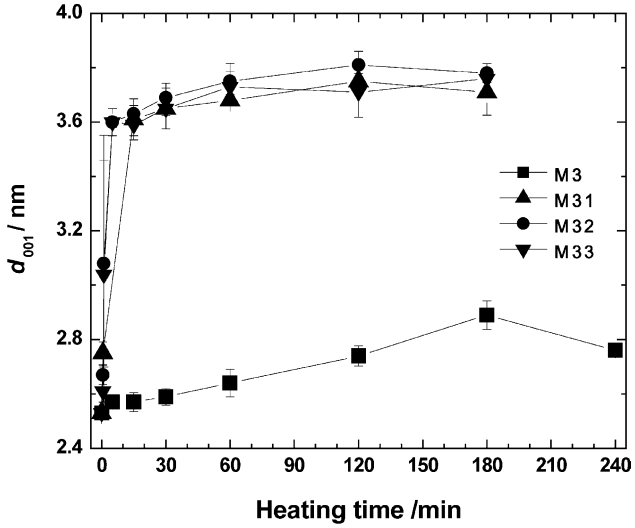


Fig. 8. Dependence of (001) interlayer spacing, $d_{001}$, of clay on heating time for M3 and M3$z$ ($z$ = 1–3) samples.

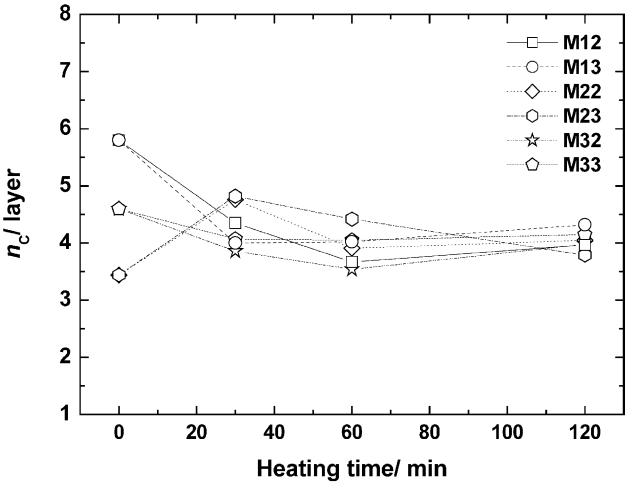


Fig. 9. Dependence of actual number of silicate layers, $n_C$, on heating time for M12, M13, M22, M23, M32, and M33 samples.

This result implies that the PLLA chains penetrate possibly into silicate galleries; the configuration of confined PLLA chains should be more planar than that of their random coil state [9].

The crystallite size normal to the (001) plane of the clay particles in PLLA matrix is calculated by the Scherrer equation [16], written as

$$h_{001} = \frac{K\lambda}{\beta \cos \theta_{001}} \quad (1)$$

where $K$ is a constant (=0.91), $\lambda$ the X-ray wavelength (= 0.154 nm), $\beta$ the width of Bragg diffraction peak determined by the full width at haft maximum in radian unit, and $\theta_{001}$ the half of (001) diffraction angle. From the calculated crystallite size ($h_{001}$), i.e. the thickness of the dispersed clay, the actual number of layers, $n_C$, staked in a clay particle can be approximately calculated as follows

$$n_C = \frac{h_{001}}{d_{001}} + 1 \quad (2)$$

Fig. 9 shows the dependence of $n_C$ on heating time for the M12, M13, M22, M23, M32, and M33 samples before and after melting process for various times. The other samples exhibit quite similar results, so it is not necessary to mention here. All the samples show that the $n_C$ values change between 3 and 6 layers, indicating that the clay particles do not have any tendency to delaminate into individual layers; in other words, the clay particles remain stacked in the PLLA matrix after the melting process.

### 3.3. Microscopic observation

Fig. 10 shows bright-field TEM micrograph for (a) M11, (b) M21, and (c) M31 samples after having been melt-processed at 190 °C for 30 min. We see that large agglomerated tactoids exist in all samples. The aggregated feature of clay particles is independent of the surfactants. An agglomerated tactoid contain many smaller primary particles, which consists of several silicate layers, and the number of which will be estimated by higher magnification TEM micrographs later. The TEM results suggest that the clay particles still stack and remain in the PLLA matrix as agglomerated tactoids via melting process without shearing force. These TEM results clarifies the dispersion structure of clay particles in PLLA and are consistent with the WAXD results. In the case of shearing force applied, the primary particles showed their much finer dispersion state in PLLA matrix with the thickness and length of individual dispersed clays of 5–12 nm and 0.5–0.7 μm, respectively, in spite of comparable $n_C$ values as compared with those in these systems [8–12]. This suggests the shearing forces play a very important role in melt compounding for dispersing clay particles in the polymer matrices.

Fig. 11 shows high magnification TEM micrographs for M12 samples after being melt-processed for (a) 30 s, (b) 30 min, and (c) 3 h. Apparently, the aggregate structure of clay particles does not change at all with increasing the heating time. The individual layers still stack in the primary particles, and many of those particles located within the large agglomerated tactoids. We find that there are 5–20 individual layers contained in one primary particle. The basal spacing observed for silicate layers in primary particles are 3.0–3.4 nm for M2$y$ samples, and 2.4–3.0 nm for M1$x$ and M3$z$ samples. These results are comparable with that obtained by WAXD.

## 4. Conclusions

In this study, we prepared the PLLA/clay compounds and investigated the melt intercalation of PLLA into clay galleries via melting process without shearing force. The results obtained are as follows

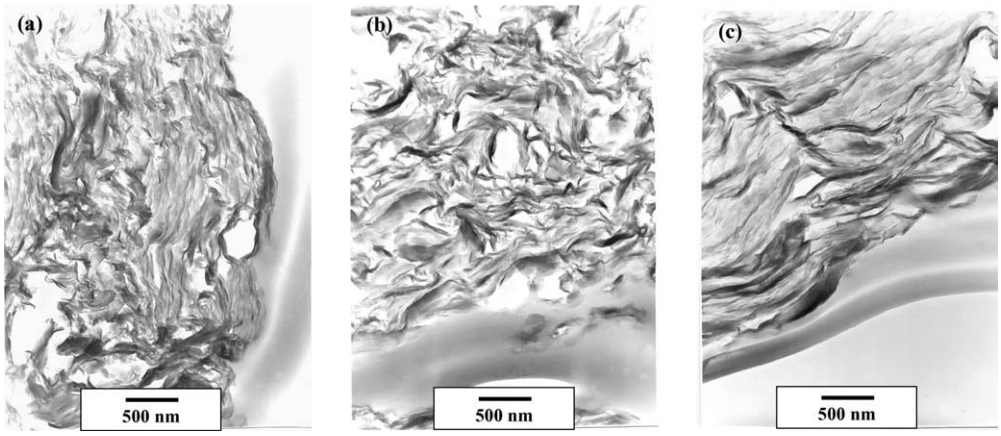


Fig. 10. Bright-field TEM micrographs showing for (a) M11, (b) M21, and (c) M31 samples after being melt-processed at 190 °C for 30 min.

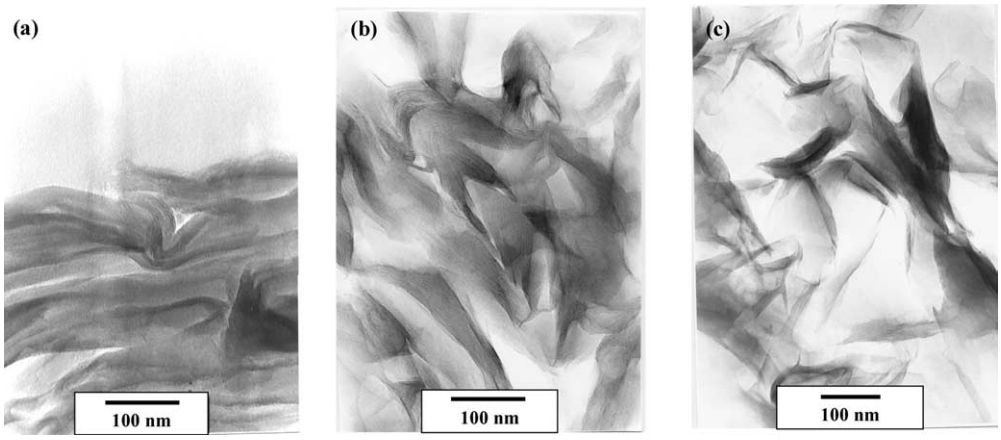


Fig. 11. Bright-field TEM micrographs showing for M21 sample after being melt-processed at 190 °C for (a) 30 s, (b) 30 min, and (c) 3 h.

(1) Under melting process, the clay particles exhibit the increase in their basal spacing $d_{001}$ in different manner for the M1$x$, M2$y$, and M3$z$ samples due to the penetration of PLLA chains into silicate galleries. With increasing heating time, the $d_{001}$ values increased more slowly for the M3$z$ samples as compared with that for the other M1$x$ and M2$y$ samples. In addition, the maximum extent of $d_{001}$ depends on clay content for the M1$x$ and M2$y$ but M3$z$ samples. The melt intercalation of PLLA is thus strongly dependent on the types of ammonium surfactants, clay content in PLLA and heating time.

(2) The clay particles do not show any tendency of delamination into individual layers and remain as large agglomerated tactoids in the PLLA matrix. The shearing force thus plays an important role in melt-compounding of polymer/clay hybrids.

## Acknowledgements

The authors highly appreciate the contributions of Mr Kazuo Sasaki of Yamagata University, who carried out some parts of the WAXD works.

## References

[1] LeBaron PC, Wang Z, Pinnavaia TJ. Appl Clay Sci 1999;15:11.
[2] Vaia RA, Price G, Ruth PN, Nguyen HT, Lichtenhan J. Appl Clay Sci 1999;15:67.
[3] Alexandre M, Dubois P. Mater Sci Eng 2000;28:1.
[4] Usuki A, Kojima Y, Okada A, Fukushima Y, Kurauchi T, Kamigaito O. J Mater Res 1993;8:1179.
[5] Kojima Y, Usuki A, Kawasumi M, Okada A, Fukushima Y, Kurauchi T, et al. J Mater Res 1993;8:1185.
[6] Vaia RA, Ishii H, Giannelis EP. Chem Mater 1993;5:1694.
[7] Vaia RA, Jandt KD, Kramer EJ, Giannelis EP. Macromolecules 1995; 28:8080.
[8] Nam PH, Fujimori A, Masuko T. e-Polymers 2004;005.
[9] Nam PH, Fujimori A, Masuko T. J Appl Polym Sci 2004;93(6):2711.
[10] Ninomiya N, Nam PH, Fujimori A, Masuko T. e-Polymers 2004;41.
[11] Nam PH, Ninomiya N, Fujimori A, Masuko T. Proceedings of 40th IUPAC international symposium on macromoecules. vol. P4.3 2004. p. 151.
[12] Ninomiya N, Nam PH, Fujimori A, Masuko T. Proc Malaysian Chem Congress 2004;143.

13 (a) Pluta M, Galeski A, Alexandre M, Paul MA, Dubois P. J Appl Polym Sci 2002;86(6):1497.
(b) Ray SS, Maiti P, Okamoto M, Yamada K, Ueda K. Macromolecules 2002;35:3104.
(c) Paul MA, Alexandre M, Degee P, Henrist C, Rulmont A, Dubois P. Polymer 2003;44:443.
(d) Ray SS, Yamada K, Okamoto M, Ueda K. Polymer 2003;44:857.
(e) Paul MA, Alexandre M, Calberg C, Jerome R, Doubois P. Macromol Rapid Commun 2003;24:561.
(f) Chang JH, An YU, Sur GS. J Polym Sci, Part B: Polym Phys 2003; 41:94.
[14] Fukushima Y. Nihonkinnzokugakkaikaihou 1990;29(3):125.
[15] Miyata T, Masuko T. Polymer 1997;38:4003.
[16] Cullity BD. Element of X-ray diffraction. Reading, MA: Addison-Wesley; 1978. p. 99.